© 2003 OSA/IPR 2003

Complex-frequency leaky mode computations using PML boundary layers for dielectric resonant structures

Miloš Popović
Research Laboratory of Electronics, Department of Electrical Engineering and Computer Science, Massachusetts Institute of Technology, Rm. 36-363, 50 Vassar St, Cambridge, MA 02139
Tel (617)253-8302, Fax (617)253-9611, milos@mit.edu

Abstract: Perfectly matched layers are used for finite-difference computation of complex-frequency leaky modes of resonant dielectric structures in cylindrical and Cartesian coordinates. Examples of dielectric-halfspace-perturbed 3D rings and 2D round, square and coupled resonators are given.
©2003 Optical Society of America
OCIS codes: (130.3120) Integrated optics devices; (130.2790) Guided waves; (000.4430) Numerical approximation and analysis; (230.5750) Resonators, (230.7370) Waveguides.

Resonant dielectric structures play an instrumental role in high-density integration of optical channel add/drop filters. Dielectric resonators coupled mutually and to waveguides can give sharp, box-like complementary bandpass and bandstop frequency responses desired in channel add/drop filters [1-2]. Resonators are also found in proposals for high index contrast (HIC) low-crosstalk crossings, sharp bends [3], and fiber-chip couplers [4].

Coupling of modes in time (CMT) has been a successful theory for dealing with coupled resonant cavity modes, e.g. in ring [1] or square resonator filters [2-4]. Complex-frequency supermodes, where the imaginary frequency component accounts for decay in the case of a finite Q, are the natural solutions which result from a CMT treatment of coupled resonators with no driving term.

A mode solver for the complex-frequency modes of a resonant structure can be used to find the individual resonator parameters (modes of interest, frequencies, Q's) for a CMT analysis. It also allows comparison of the exact supermodes with the CMT result. Studying the mode structure gives insight into the physical operation of the device and can be of help in fine-tuning the predictions of approximate analytic methods like CMT. Some effects of resonator coupling not usually included in first-order CMT include self-frequency shift and a modified radiation Q. These are accessible to computation.

Energy modes of dielectric resonators, even in lossless dielectric media, have a fundamental radiation loss – a finite unloaded Q. Thus methods to compute them must handle outgoing radiation and a complex resonant frequency representative of the decay, where $Q \equiv -\omega_R / 2\omega_I$ (Q > 0 for loss).

We present the use of PML boundary layers [5] in the direct computation of leaky mode complex frequencies and field distributions for dielectric resonant structures. The full-vector Maxwell's equations for the transverse electric field, cast as an eigenvalue problem with complex-frequency (squared) eigenvalue, are solved on a 2D domain of interest bound by radiation-absorbing PMLs. Here, the domain can be a ρ-z cross-section of a cylindrically symmetric 3D resonant structure, or the x-y plane of a 2D resonant system.

The cylindrical finite-difference (FD) formulation in this paper is on the Yee grid as FDTD [6], but in the frequency domain as in [7]. PMLs, extended to cylindrical coordinates in [8], are used to pad the edges of the computational domain. Huang et al. first applied PMLs to a 1D, Cartesian complex propagation constant FD modesolver [9].

Using Chew's notation [10] for difference equations on the Yee grid, the cylindrical-geometry eigenvalue equation solved here for leaky modes is (assuming a diagonal, spatially-varying ε-tensor and a constant, scalar μ)

$$\left[\begin{array}{c|c} -\hat\partial_z\tilde\partial_z - \frac{1}{\rho^2_{m+\frac12}}\tilde\partial_\rho \frac{\rho_m}{\epsilon^{\phi\phi}_{\mathbf m}}\hat\partial_\rho \rho_{m+\frac12}\epsilon^{\rho\rho}_{\mathbf m} & \hat\partial_z \frac{1}{\rho_{m+\frac12}}\tilde\partial_\rho\rho_m - \frac{1}{\rho^2_{m+\frac12}}\tilde\partial_\rho\frac{\rho_m^2}{\epsilon^{\phi\phi}_{\mathbf m}}\hat\partial_z\epsilon^{zz}_{\mathbf m} \\ \hline \frac{1}{\rho_m}\hat\partial_\rho\rho_{m+\frac12}\tilde\partial_z - \frac{1}{\rho_m}\tilde\partial_z\frac{1}{\epsilon^{\phi\phi}_{\mathbf m}}\hat\partial_\rho\rho_{m+\frac12}\epsilon^{\rho\rho}_{\mathbf m} & -\frac{1}{\rho_m}\hat\partial_\rho\rho_{m+\frac12}\tilde\partial_\rho - \frac{1}{\rho_m}\tilde\partial_z\frac{\rho_m}{\epsilon^{\phi\phi}_{\mathbf m}}\hat\partial_z\epsilon^{zz}_{\mathbf m} \end{array}\right] \cdot \left[\begin{array}{c} E^\rho_{m+\frac12,n} \\ E^z_{m,n+\frac12} \end{array}\right] = \\ = \left(\omega^2\mu\left[\begin{array}{c|c} \epsilon^{\rho\rho}_{\mathbf m} & \\ \hline & \epsilon^{zz}_{\mathbf m}\end{array}\right] - \gamma^2\left[\begin{array}{c|c} \frac{1}{\rho^2_{m+\frac12}} & \\ \hline & \frac{1}{\rho_m}\end{array}\right]\right)\cdot\left[\begin{array}{c} E^\rho_{m+\frac12,n} \\ E^z_{m,n+\frac12} \end{array}\right]. \quad (1)$$

Grid points are marked by **m** = (m,n), (m+½,n) or (m,n+½) in the 2D domain; the tilde (~) and caret (^) identify forward and backward differences [10]. γ is the angular propagation constant of a mode of the cylindrical structure,

© 2003 OSA/IPR 2003

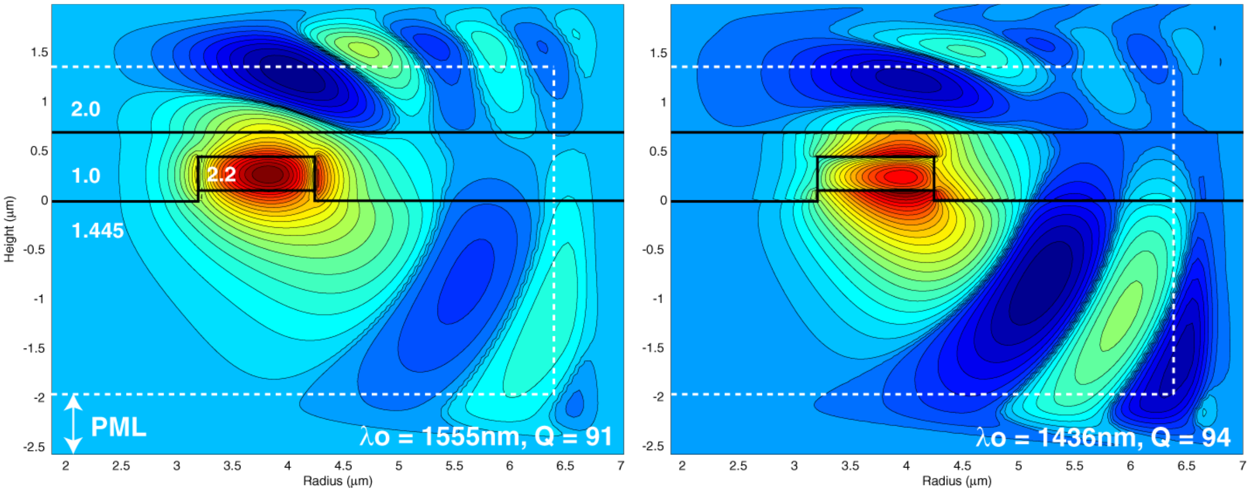

Fig. 1. Leaky modes of 3D ring resonator in proximity to a high index halfspace: (a) E_ρ of TE-like mode, (b) E_z of TM-like mode. Contours assigned quadratic spacing to show more low-amplitude detail.

and equals the order of the resonance. ω is the resonant frequency. ρ and z are interpreted as complex coordinates, as defined in [8].

For complex-frequency modes, equation (1) is rearranged so that ω^2 is the eigenvalue on the RHS of the equation. By rearranging to isolate γ^2 instead, a complex-propagation-constant eigenvalue problem for power modes is obtained. This application to full-vector complex-β modes of bent waveguides in cylindrical coordinates was independently published recently by Feng et al. [11]. In view of this publication, we will focus primarily on the complex-frequency modes here.

The eigenmode equation (1) is adapted to Cartesian geometry if one interprets z as y, ϕ as z, γ as β, and ρ as x in the derivatives only and $\rho \equiv 1$ elsewhere.

The utility of this mode solver is demonstrated with a number of examples of practical interest. The structures shown are designed for low Q, such that radiation absorbed by the PML is visible in the plots. In practice, of course, high Q is desirable.

The first example given is a 3D air-clad ring resonator on a pedestal (Fig. 1), perturbed by a high-index dielectric halfspace in proximity. The ring could be part of a coupled-ring channel add/drop filter, e.g. of a topology as in [1]. The core and cladding indices are 2.2 and 1.445, and the waveguide dimensions are a 1.05µm width, 0.33µm core height on a pedestal 0.1µm above the cladding surface, and a 4.25µm outer radius. In the absence of the dielectric, the resonant frequency of the TE-like mode is 1552nm with a radiation Q of 1706 (not shown). Lowering the high-index (n=2.0) dielectric halfspace to a 250nm displacement produces a second leakage path (Fig. 1a). The loss Q is reduced to 91, with a small shift in the resonant frequency to 1555nm. The TM-like mode in Fig. 1b experiences a slightly smaller effect due to polarization charge screening; its Q drops from 153 to 94, becoming the "lower loss" mode.

Other interesting 3D cylindrical examples will be shown in the presentation, including coupled rings and straight and bent air trench waveguides [12] with bending and substrate leakage loss.

Small resonators (a few wavelengths in size) of various geometric shapes are of interest in high index contrast [3-4]. In the second set of examples, we show the standalone TM modes of a disk and square resonator in 2D, and investigate the self-frequency shift, frequency splitting and loss-Q modification of a coupled resonator pair. This is accomplished by adapting the complex-frequency solver to Cartesian coordinates as explained above, and setting the propagation constant γ (i.e. β) to zero.

Figs. 2a,d show one of two degenerate high-Q modes near 1550nm of a disk of diameter 1.66µm (index 3:1), and a lower-Q mode chosen to show the PML absorbing outward radiation. Resonant frequencies are 1623.5nm and 1453.8 nm, with Q's of 2238 and 91. Figs. 2b,e shows coupled disks spaced by 1/10 of their diameter, 0.166µm. Four relevant modes are now found, symmetric and antisymmetric about the x and y axis. The new resonant frequencies are all different: (1611.9, 1611.1nm) and (1618.5, 1619.7nm). The major frequency splitting due to coupling of the resonators is seen between pairs of the supermodes. However, the smaller frequency difference within the pairs indicates reflection and backward coupling. Circulating traveling waves are not modes of the new

© 2003 OSA/IPR 2003

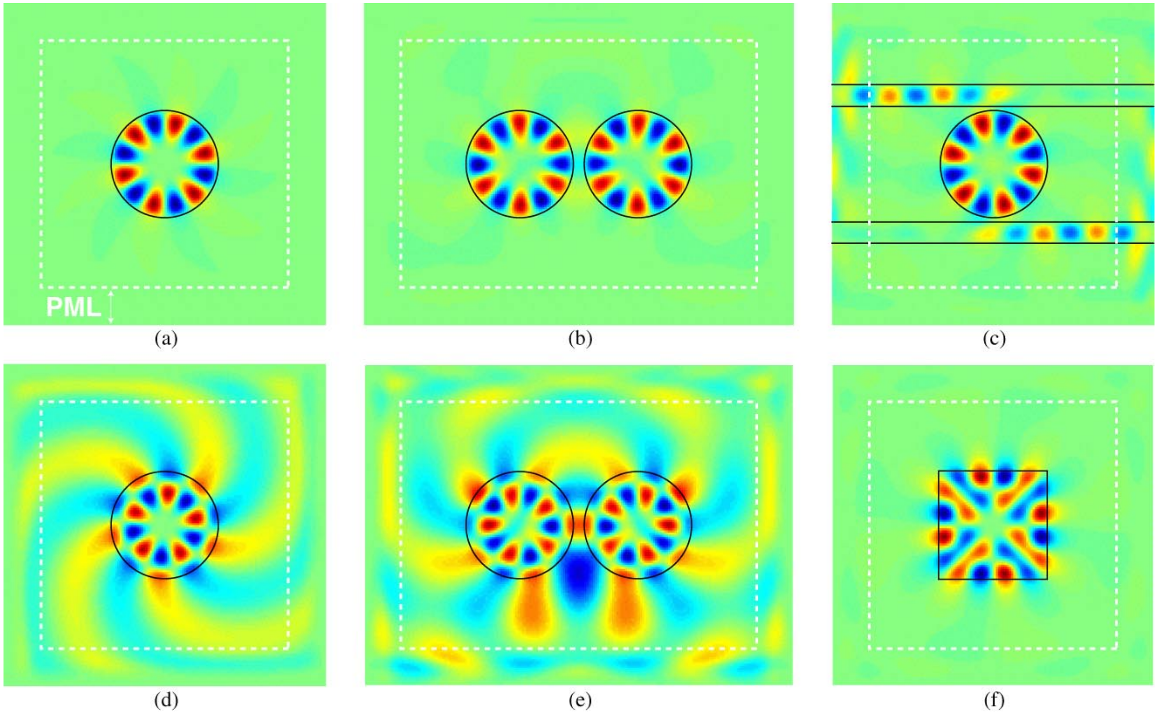

Fig. 2. Leaky modes of 2D resonators (TM, H_z field): (a) high-Q disk mode, (b) high-Q coupled-disk supermode, (c) waveguide-loaded disk mode, (d) low-Q disk mode, (e) low-Q coupled-disk supermode, (f) high-Q square resonator mode (TE, E_z).

structure, so traveling wave coupling will have an inherent loss. This effect is only pronounced in the large index contrast and strong coupling demonstrated here for illustration.

In Fig. 2c, the superposition of two almost degenerate leaky modes of a loaded resonator shows decay of power from the resonator primarily through coupled waveguides in the counter-clockwise direction. The resulting Q of ~150 is the so-called external Q, much lower than the unloaded Q above. The degeneracy of the even and odd standing wave modes is broken by the presence of the waveguides, and their resonant frequencies are shifted to 1626.9 nm and 1627.8 nm. Neither the shift nor the frequency splitting is predicted by first-order CMT, which only gives a change in the total Q. There is a fundamental back-reflection in a ring channel-drop filter.

Fig. 2f shows a standing mode of a square resonator (edge 1.66μm, index 3:1) proposed in [4]. The high-Q mode is found to be at 1556nm with a Q of 2800 for TE, matching the result in [4], and at 1415nm for TM with a Q of 4800. Other examples will be shown.

References

1. B.E. Little, S.T. Chu, H.A. Haus, J.S. Foresi and J.-P. Laine, "Microring resonator channel dropping filters," J. Lightwave Technol. **15**, 998-1005 (1997).
2. M.J. Khan, C. Manolatou, S. Fan, P.R. Villeneuve, H.A. Haus and J.D. Joannopoulos, "Mode coupling analysis of multipole symmetric resonant add/drop filters," IEEE J. Quant. Electron., **35**, 1451-1460 (1999).
3. C. Manolatou, S.G. Johnson, S. Fan, P.R. Villeneuve, H.A. Haus and J.D. Joannopoulos, "High-density integrated optics," J. Lightwave Technol., **17**, 1682-1692 (1999).
4. C. Manolatou and H.A. Haus, *Passive components for dense optical integration* (Kluwer Academic, 2001).
5. J.P. Berenger, "A perfectly matched layer for the absorption of electromagnetic waves," J. Comp. Phys., **114**, 185-200 (1994).
6. A. Taflove, *Computational electrodynamics: the finite-difference time-domain method* (Artech House, Boston, 1995).
7. K. Radhakrishnan and W.C. Chew, "An efficient Krylov-subspace-based algorithm to solve the dielectric-waveguide problem," IEEE Trans. on Microwave Theory and Tech., **49**, 1345–1348 (2001).
8. F.L. Teixeira and W.C. Chew, "PML-FDTD in cylindrical and spherical grids," IEEE Microwave and Guided Wave Lett., **7**, 285-287 (1997).
9. W.P. Huang, C.L. Xu, W.W. Lui and K. Yokoyama, "The perfectly matched layer boundary condition for modal analysis of optical waveguides: Leaky mode calculations," IEEE Photon. Technol. Lett., **8**, 652-654 (1996).
10. W.C. Chew. "Electromagnetic theory on a lattice," J. Applied Phys., **75**, 4843–4850 (1994).
11. N.N. Feng, G.R. Zhou, C. Xu, and W.P. Huang, "Computation of full-vector modes for bending waveguide using cylindrical perfectly matched layers," J. Lightwave Technol., **20**, 1976-1980 (2002).
12. M. Popović, K. Wada, S. Akiyama, H.A. Haus and J. Michel, "Air trenches for sharp silica waveguide bends," J. Lightwave Technol., **20**, 1762-1772 (2002).